Journal of Sound and Vibration (1990) 137(3), 357-368

BISPECTRAL ANALYSIS OF SYSTEMS POSSESSING CHAOTIC MOTION

C. PEZESHKI

Department of Mechanical and Materials Engineering,

S. ELGAR

Department of Electrical and Computer Engineering,

AND

R. C. KRISHNA

Department of Mechanical and Materials Engineering, Washington State University, Pullman, 99164-2920, U.S.A.

(*Received* 27 *February* 1989)

Bispectral analyses of the equations producing a chaotic Rossler attractor and the chaotic trajectories of a one-mode Galerkin approximation of the magnetically buckled beam are presented, yielding interesting consequences concerning chaotic system identification for driven oscillators and autonomous systems. Bicoherence spectra isolate the phase coupling between increasing numbers of triads of Fourier modes for a pure period doubling sequence route to chaos for the Rossler equations. Bicoherences from a period doubling-intermittency catastrophe route to chaotic motion are also observed for single frequency excitation for the buckled beam. Although the bicoherence successfully characterizes important aspects of the non-linearity of the Rossler attractor in the nonchaotic and chaotic regimes, where the primary non-linearity is quadratic, it only partially characterizes the magnetically buckled beam system because the dominant non-linearity is cubic.

1. INTRODUCTION

Since their introduction more than 25 years ago [1], bispectral and other polyspectral techniques have been used to study a wide variety of non-linear systems, including fluid mechanics [2-8], mechanical systems analysis [9, 10], and quantum mechanics [11] (see reference [12] for a recent review).

It is well known that although power spectral analysis is adequate for investigating aspects of linear systems, power spectra do not contain phase information, and thus cannot be used to study non-linear interactions between Fourier modes. On the other hand, higher order spectra isolate phase coupling between non-linearly interacting Fourier components. In the present study, bispectral analysis is used to investigate the quadratic interactions that produce a pure period-doubling sequence to chaos in the Rossler equations [13, 14]. Period doubling and other quadratic phenomena also play an important role in the dynamics of the buckled beam [15, 16], and this system is studied here with bispectral techniques.

Application of spectral techniques to non-linear systems is of vital importance to engineers in the field. Frequency spectra are easily calculated measures of a system's dynamics. However, for complex non-linear systems, information about non-linear modal coupling in the system is lost due to the phase information-destructive nature of power

0022-460X/90/060357+12 $03.00/0

spectral calculations. This can particularly affect analysis of chaotic systems, which possess continuous frequency spectra with coupled harmonic content, but can be incorrectly characterized as linear systems containing several strong harmonics coupled with a random element, with the consequent ignoring of non-linear frequency coupling. This incorrect diagnosis of the motion may lead to suggesting inappropriate design changes since the true nature of the behavior has been misinterpreted.

Polyspectral techniques, notably bispectra, offer a method of analyzing modal interactions in non-linear systems. This knowledge can be very important in non-linear structural dynamical systems, in that certain types of damping and stiffness possess quadratic form. Consequently, bispectral analysis can be used by an engineer in the field to analyze a complicated non-linear system and improve its design.

Other quantitative measures of non-linear systems exist, such as the fractal dimension [17–20 and others]. The concept of fractal dimension for non-linear dynamical systems has allowed an infinite-order continuous system to be represented in lower-dimensional phase spaces by a finite number of degrees of freedom. There are many different ways of measuring dimension for lower order systems from experimental data, including the Grassberger–Procaccia, or correlation, dimension [18–20], the averaged pointwise dimension [21], and the Lyapunov dimension [22].

The calculation of fractal dimension of chaotic attractors offers one way of investigating their low-level modal structure. Typically, the phase space is reconstructed from the time series by using the method of delays [21]. The fractal dimension gives a rough estimate of the necessary size of the phase space for the attractor to be topologically complete, and thus is of value to engineers because it provides an estimate of the number of degrees of freedom that an engineering system possesses.

Although the fractal dimension estimates the number of non-linear modes, many of the modes are not analytic or estimable by any standardized procedure. It has been shown that the number of phase space variables derived from linear modes that are necessary to accurately represent physical behavior of the buckled beam system appears to be the same as the estimated Lyapunov dimension [23]. This is convenient for the buckled beam, because the linear system modes are probably very close in structure to the non-linear modes. However, this rule of thumb is not necessarily true for other systems. Although the fractal dimension may indicate that the problem of vibrations in a system with a broadband power spectrum is tractable since there actually are only a finite number of degrees of freedom, these dimensions do not yield the specific information about mode coupling necessary for an engineer to "fix" the problem at hand.

Another quantitative measure of non-linear systems is the Lyapunov exponent [24 and references therein]. Lyapunov exponents are good measures of system instability, and can yield insight into system behavior [23]; they are also useful because they give an eigenvalue equivalent that can be compared to any linear system analysis. Lyapunov exponents are essentially the real parts of non-linear eigenvalues for a given attractor and, as such, give qualitative information on an attractor's dynamics. For example, chaotic attractors existing in a three-dimensional phase space have one positive, one zero and one negative Lyapunov exponent. Lyapunov exponents are also one of the few techniques that give a quantitative measure of chaos. By using the conjecture of Kaplan and Yorke [22], an estimate of fractal dimension can also be calculated from the exponents.

Although the methods of modern non-linear dynamics have been very valuable in the understanding of non-linear systems, they do not present detailed information about non-linear mode coupling on a frequency by frequency basis. Such frequency domain information is necessary in order to prescribe actions to affect gross portions of the spectrum, such as attenuating harmonics in a particular frequency range. Bispectral

analysis offers a method for determining the non-linear coupling between Fourier modes, and explains the origins of spectral peaks at certain values in the frequency spectrum. With the information provided by the bispectrum, an engineer could take precautions to damp out the root frequencies causing the unwanted oscillations, instead of the frequency that results from the non-linear interaction.

Definitions of relevant bispectral quantities and details of the numerics are briefly presented in section 2. Bicoherence spectra for the Rossler attractor and the magnetically buckled beam are presented in section 3. The quadratic interactions resulting in the period-doubling sequence to chaos of the Rossler attractor are isolated by the bispectrum. Bispectra also provide useful information about mode coupling as the buckled beam oscillations approach chaos. For the fully chaotic buckled beam case, bicoherence spectra indicate that quadratic non-linear oscillations no longer dominate, consistent with the cubic nature of the governing equation. Conclusions are presented in section 4.

2. BISPECTRAL ANALYSIS AND NUMERICAL DETAILS

For a discretely sampled time series $\eta(t)$ with the Fourier representation

$$\eta(t) = \sum_n A(\omega_n)\, e^{i\omega_n t} + A^*(\omega_n)\, e^{-i\omega_n t} \tag{1}$$

the power spectrum and the auto-bispectrum are defined respectively as

$$P(\omega_1) = E[A(\omega_1)A^*(\omega_1)], \qquad B(\omega_1, \omega_2) = E[A(\omega_1)A(\omega_2)A^*(\omega_1+\omega_2)], \tag{2,3}$$

where ω_n is the radian frequency, the subscript n is a frequency index, the As are the complex Fourier coefficients of the time series, an asterisk indicates complex conjugate, and E [ ] is the expected value, or average, operator. The normalized magnitude of the bispectrum, known as the squared bicoherence, is given by

$$b^2(\omega_1, \omega_2) = |B(\omega_1, \omega_2)|^2 / P(\omega_1)P(\omega_2)P(\omega_1+\omega_2). \tag{4}$$

It is well known that b^2 represents the fraction of power at the sum frequency $(\omega_1+\omega_2)$ of the triad owing to quadratic interactions between the other Fourier modes ω_1 and ω_2 [25]. For a digital time series with Nyquist frequency ω_N, the auto-bicoherence is completely described by values within a triangle with vertices at $(\omega_1 = 0,\ \omega_2 = 0)$, $(\omega_1 = \omega_{N/2},\ \omega_2 = \omega_{N/2})$, and $(\omega_1 = \omega_N,\ \omega_2 = \omega_0)$ [1].

The time series analyzed here were numerically generated on an IBM 3090. The Rossler equations were numerically integrated by using a classic fourth order Runge-Kutta subroutine, with a time step of 0·001 s for a system with a fundamental period of 12·5 s. The resulting 3276 s long time series were sampled at 10 Hz for power spectral and bispectral analysis. Subsections of 51·2 s duration were fast Fourier transformed to yield the complex Fourier coefficients $A(\omega_n)$ with a frequency resolution of 0·0195 Hz. Power and auto-bispectra were calculated for each 51·2 s and then were ensemble averaged over the collection of 64 subsections, producing estimates with 128 degrees of freedom. The Duffing equation used to represent the magnetically buckled beam (section 3) was numerically integrated by using the same subroutine with a time step of 0·015 s. The resulting 4096 s long time series were sampled at 1 Hz and subdivided in 32 segments of 128 s duration for processing, resulting in a frequency resolution of 0·0078 Hz and 64 degrees of freedom. Tests with different length data segments and windows indicated that the rectangular windows of 51·2 and 128 s did not result in significant spectral or bispectral leakage or smearing for the data considered here. Bicoherence values of $b > 0{\cdot}22$ and

$b > 0{\cdot}31$ are statistically significant at the 95% level for 128 and 64 degrees of freedom, respectively [26].

3. RESULTS

In this section phase plane portraits, power spectra and bicoherence spectra for the Rossler attractor and the magnetically buckled beam are presented.

3.1. THE ROSSLER ATTRACTOR

The equations for the Rossler attractor are models of the Lorenz attractor [14], which is a modal reduction for Rayleigh–Bernard convection:

$$\dot{X} = -(Y+Z),$$

$$\dot{Y} = X + Y/5, \qquad \dot{Z} = \tfrac{1}{5} + Z(X-\mu). \tag{5}$$

The Rossler attractor provides the simplest non-linear vector field capable of producing the folding nature necessary for chaotic dynamics [14]. These equations, taken from reference [13], are autonomous and possess only a single quadratic non-linearity.

The parameters that generate a period-doubling sequence and chaos are well documented (see reference [13]) and are listed in Figure 1. Although the period doubling route to chaos of the Rossler attractor has been studied [14], the bispectral analysis isolating the non-linearly coupled triads of Fourier modes has not been previously reported. As discussed above, ordinary power spectral analysis cannot provide information on phase coupling between modes, nor on the cross-spectral transfer of energy between motions at the primary spectral peak frequency and its motions at sub- and super-harmonics. On the other hand, since the equations describing the Rossler attractor are quadratically non-linear, bispectral analysis is an appropriate tool with which to study the coupling of and energy exchange between the various modes of the system.

Phase plane portraits for period one, period two and chaotic attractors of the Rossler system are shown in Figure 1. Corresponding power spectra are shown in Figure 2 and are characterized by narrow spectral peaks. The harmonic structure of the Rossler attractor is clearly displayed in the power spectra (Figure 2). For one-period motion, the spectrum is dominated by a primary spectral peak located at $f = 0{\cdot}17$ Hz, and its higher harmonics. As μ is increased, the subharmonic ($f = 0{\cdot}085$ Hz) is excited and, owing to the quadratic non-linearities, the spectrum contains peaks at frequencies corresponding to sum interactions of the subharmonic, the primary and their harmonics. As μ is increased further, the motion becomes chaotic, as demonstrated by the phase portrait (Figure 1(c)) and the broadening of the power spectrum (Figure 2(c)).

The quadratic interactions between triads of Fourier modes for the Rossler attractor are shown in Figure 3. For the period one case, bicoherence spectra (Figure 3(a)) clearly show the coupling between motions at the primary spectral peak frequency and its harmonics, as well as between the first and second harmonic, the first and third, the second and itself, and further on out into the higher frequencies. The strong band of bicoherence associated with $f = 0{\cdot}17$ Hz indicates non-linear energy transfer from the primary to the higher frequency modes.

Power spectra of the period doubling case (Figure 2(b)) show narrow peaks between, and somewhat higher in level than, the harmonics of the primary peak. The corresponding bicoherence spectrum (Figure 3(b)) shows the coupling between motions at the primary peak frequency, its harmonics, the period doubled frequency and its harmonics. The dominant frequencies causing the quadratic interactions now appear to be the primary

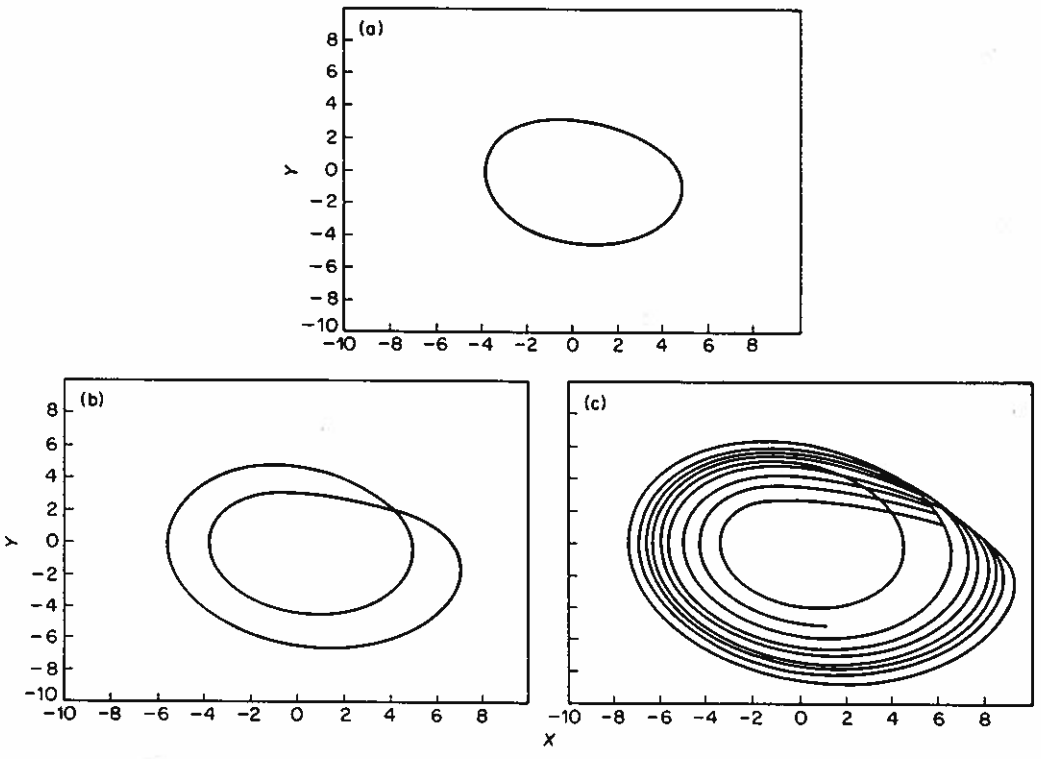

Figure 1. Phase portraits for the Rossler attractor, $Y(t)$ *vs.* $X(t)$: (a) period 1 motion, $\mu = 2{\cdot}6$; (b) period-doubled motion, $\mu = 3{\cdot}5$; (*c*) chaotic motion, $\mu = 4.6$.

spectral peak frequency and the period doubled harmonic. Interactions between these modes are again transferring energy into the higher harmonics, giving a greater number of peaks in the frequency spectrum with a much richer structure than the period one case. The strong interactions of the primary with itself, the period doubled subharmonic, and the higher harmonics are clearly shown in the bicoherence spectrum.

Bicoherences for chaotic motion for the Rossler attractor (Figure 3(c)) are very similar to the period-doubled attractor, with many of the same harmonic relationships. In addition, there is much greater bicoherence between the period-doubled subharmonic and the higher harmonics. The main energy source for the motion is the primary frequency, and a band of high bicoherence is starting to appear, originating from the fundamental frequency. The fact that the Rossler attractor in the chaotic range has strong bicoherence strongly supports the possibility of using higher order spectra for chaotic system identification in the field.

3.2. THE MAGNETICALLY BUCKLED BEAM

For the magnetically buckled beam (Figure 4), it is useful to think in physical terms. The magnetically buckled beam is often referred to as a two-well potential problem. At rest, the physical system has two stable equilibria, one buckled about the left magnet, and the other about the right magnet. It also has one unstable equilibrium, located about the center of the two magnets. If the beam is excited with a small sinusoidal force, it will oscillate about one of the two stable equilibria in a roughly sinusoidal fashion. However, as the force amplitude is increased, the beam will jump back and forth between the two static equilibria, in effect "snapping through" the centerline of the system. If the motion

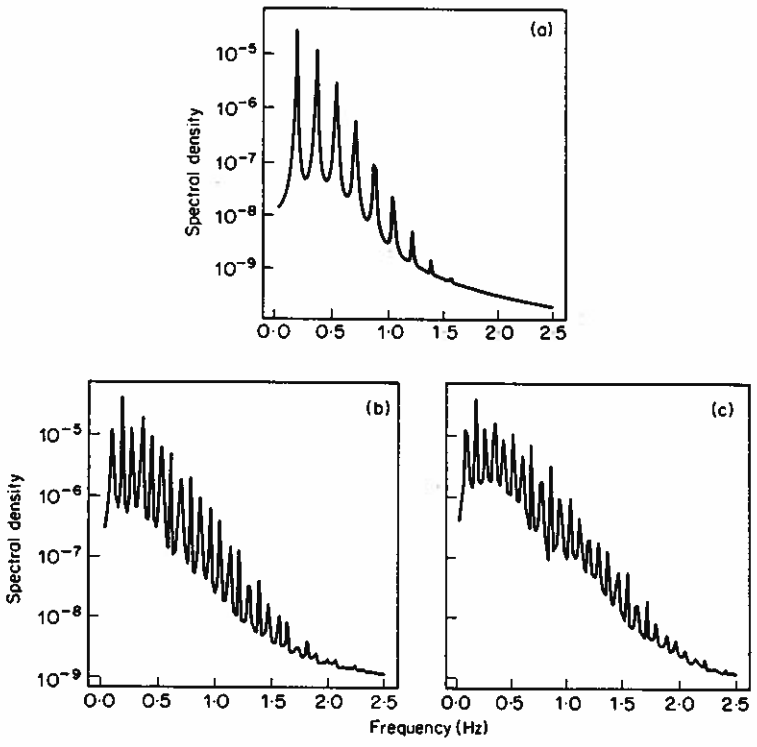

Figure 2. Power spectra for the Rossler attractor. (a) Period 1 motion; (b) period-doubling motion; (c) chaotic motion. The units of power are arbitrary.

is chaotic, as it often is if the beam is flexible and lightly damped, the beam snaps through at apparently random times, wandering back and forth between the two equilibria.

The procedure used here to analyze the magnetically buckled beam consists of examining trajectories generated by a Rayleigh–Ritz approximation to the system, given by [15]

$$\ddot{X} + \gamma\dot{X} - \tfrac{1}{2}(X - X^3) = F\cos\omega t, \tag{6}$$

where $\gamma = 0{\cdot}168$ and $\omega = 1$. This equation is commonly referred to as a Duffing equation with a negative linear stiffness, and is a linear second order equation with non-linear cubic terms attached. This equation yields a rich set of highly non-linear behavior, including strongly and weakly chaotic motions [27, 28].

Since the beam's behavior is non-linear, there exists a strong set of modal couplings that previously have not been studied by using bispectral techniques. As discussed above, ordinary power spectra do not preserve the information about energy exchange and phase coupling between sub- and superharmonics of the non-linear beam motion. Bispectral analysis adds the necessary "missing link" to previous analysis techniques because it can show how the dominant oscillating frequencies present in the non-linear beam are coupled.

Phase plane portraits of the limit cycles of the Duffing equation as it undergoes a period-doubling sequence to chaos for the single frequency excitation case are shown in Figure 5. This cascade ends with a well documented saddle node bifurcation catastrophe with intermittency [14] leading to the chaotic attractor shown in Figure 5(d). A Poincaré map of the chaotic attractor is shown in Figure 6 and power spectra corresponding to the phase portraits are shown in Figure 7. The Poincaré sampling occurs every period of the forcing function oscillation. The period one spectrum (Figure 7(a)) consists of one

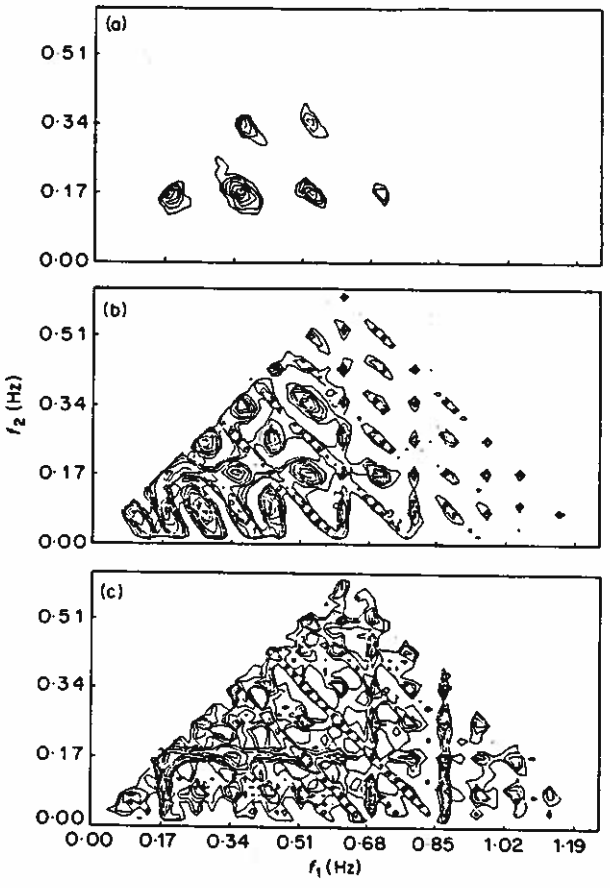

Figure 3. Contours of bicoherence for the Rossler attractor. f_1 and f_2 are shown, while the sum frequency, f_1+f_2, is implied. The minimum value of bicoherence plotted is $b=0{\cdot}3$, with contours every 0·1.

broad primary peak located at $f=0{\cdot}16$ Hz and its superharmonic; the period two spectrum (Figure 7(b)) shows a subharmonic peak at 0·08 Hz, half the driving frequency, as well as some new superharmonics, and the period four spectrum (Figure 7(c)) develops an additional peak at approximately 0·04 Hz, as well as a new range of superharmonics. When the system becomes chaotic, the power spectrum becomes quite broadband, with large amounts of very low frequency energy (Figure 7(d)).

Bicoherence spectra for the four cases are shown in Figure 8. As shown in Figure 8, the coupling between Fourier modes starts out centered about the dominant frequencies composing the limit cycles. As the force amplitude is increased, resulting in period doubling, motions at additional frequencies are excited (e.g., Figure 7(b)) by quadratic interactions between the dominant frequency and itself, as well as smaller interactions between the superharmonics. The bicoherences of the period-quadrupled limit cycle (Figure 8(c)) show the increased number of quadratic interactions for this case. Once again, there is strong bicoherence where the dominant frequency interacts with itself, as well as a spreading in the bicoherence pattern where motions at many of the superharmonic and subharmonic frequencies are interacting with each other (Figure 8(c)). The bicoherences in Figures 8(a)-(c) are spread in large clusters, owing to the width of the peaks in the power spectra (Figures 7(a)-(c)). Frequencies on either side of a respective peak interact with each other, creating this spreading.

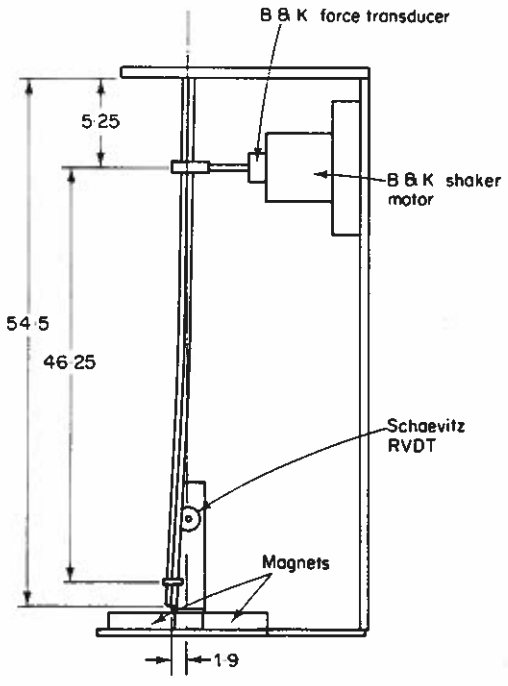

Figure 4. Magnetically buckled beam. All dimensions in cm.

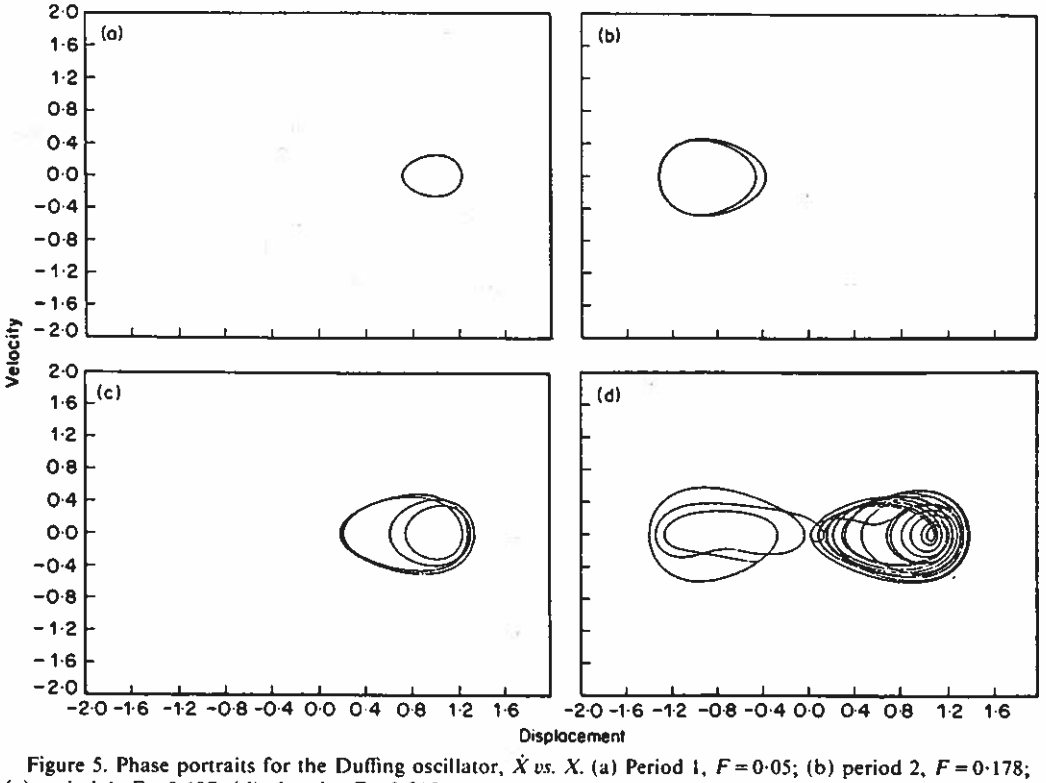

Figure 5. Phase portraits for the Duffing oscillator, $\dot{X}$ *vs.* X. (a) Period 1, $F = 0{\cdot}05$; (b) period 2, $F = 0{\cdot}178$; (c) period 4, $F = 0{\cdot}197$; (d) chaotic, $F = 0{\cdot}210$.

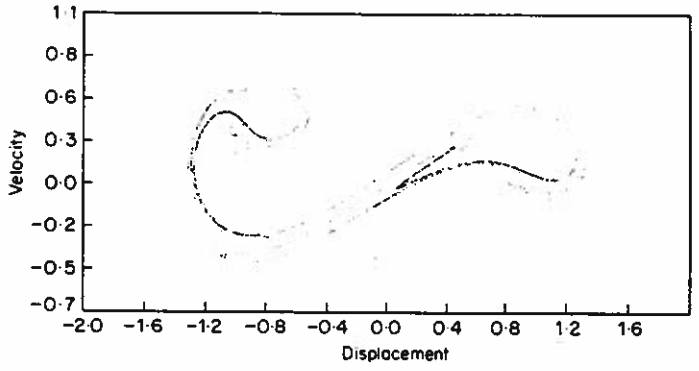

Figure 6. Poincaré map for chaotic Duffing oscillator.

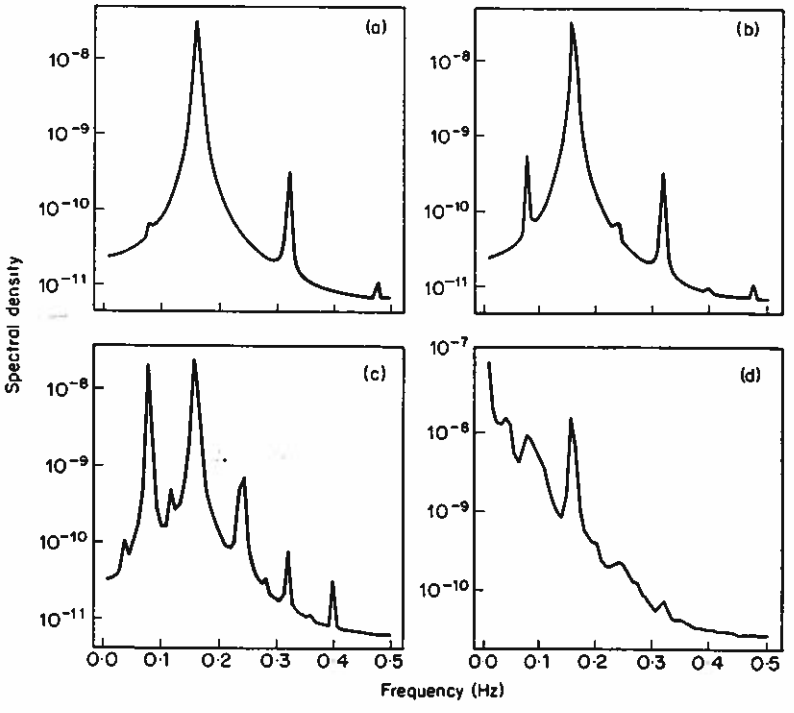

Figure 7. Power spectra for Duffing oscillator: (a) period 1; (b) period 2; (c) period 4; (d) chaotic; units of power are arbitrary.

Once the motion enters the chaotic regime (Figures 5(d), 6, 7(d) and 8(d)), the bicoherence diffuses and diminishes. This is because the dominant chaotic mechanism in the buckled beam is not a quadratic phenomenon. The beam undergoes an intermittency crisis and begins oscillating back and forth between both static equilibria. Since the motion is global in nature, the cubic term will now dominate the motion, thus leaving only an insignificant amount of quadratic phase coupling and energy transfer in the beam's motion. Similar behavior has been observed in bispectra of the driven Sine-Gordon chain [11]. Trispectral techniques (in progress) are required to analyze the higher order non-linear interactions that dominate the chaotic behavior of cubic systems such as the Duffing and Sine-Gordon attractors.

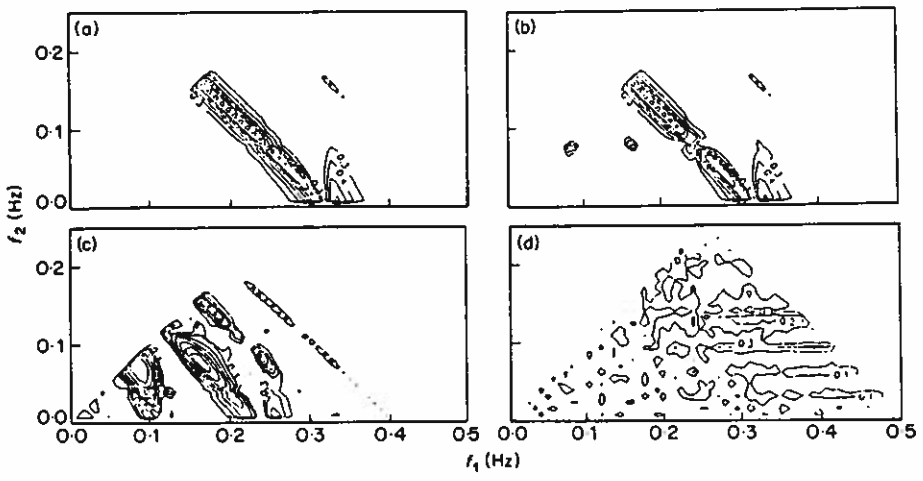

Figure 8. Contours of bicoherence for Duffing oscillator: (a) period 1; (b) period 2; (c) period 4; (d) chaotic; minimum contour is $b = 0{\cdot}3$, with contours every 0·1.

Lyapunov exponents for the transition into chaotic behavior are shown for the magnetically buckled beam in Figure 9. Lyapunov exponents are determined by examining the long-term evolution of an infinitesimal n-sphere of initial conditions, with n being the order of the non-linear system. As the system evolves, the initial n-sphere will expand or contract along its n principal axes, creating a deformed n-ellipsoid. The Lyapunov exponents for a given ellipsoidal principal axis $p_i(t)$ are defined as [24]

$$\lambda_i = \lim_{t \to \infty} (1/t) \log_2 \{p_i(t)/p_0(t)\}.$$

Although the Lyapunov exponents do document the chaotic transition, and show the period-doubling points clearly by the existence of a zero Lyapunov exponent, they do not offer any frequency information. In a sense, a combination of Lyapunov exponents and higher order spectra offer a complete description of a non-linear system; the Lyapunov exponents serving as the real part of the non-linear eigenvalue, the higher order spectra showing the groups of frequencies and their interrelationships.

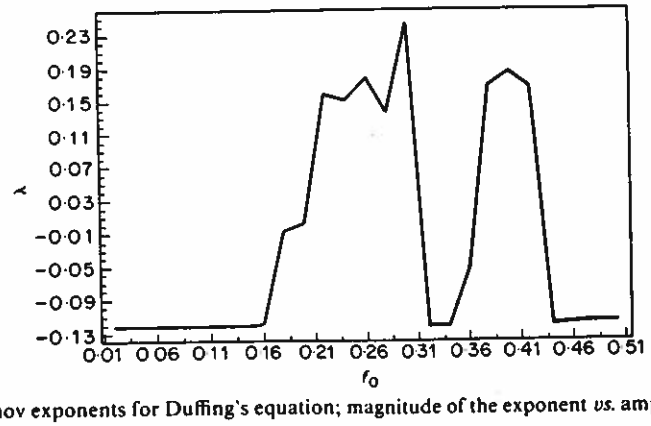

Figure 9. Lyapunov exponents for Duffing's equation; magnitude of the exponent *vs.* amplitude of the forcing function.

4. CONCLUSIONS

Bicoherence calculations were performed on a period-doubling cascade for the Rossler equations and the Duffing oscillator. The non-linear interactions of the Rossler equations, possessing only a quadratic non-linearity, are completely characterized by bicoherence both outside the chaotic regime and into it. The calculated period one, two and chaotic trajectories all possessed strong bicoherence originating primarily about the fundamental frequency of oscillation. This shows that systems possessing chaotic motions originating from quadratic interactions can successfully be characterized by bispectral techniques.

The bicoherence of the period-doubled limit cycles for the Duffing oscillator also proved to be useful in explaining the mechanics of the period-doubling process by showing which frequencies were interacting quadratically and the degree of that interaction. However, upon transition to the chaotic regime, the bicoherence present in the Duffing oscillator vanished, owing to cubic rather than quadratic interactions that caused an intermittency crisis in the oscillator.

The analysis presented here is important because polyspectral methods, like power spectra, operate solely on time series information. Thus, experimental data can be as easily analyzed as trajectories generated by computer simulation. Because of the results with both oscillators, it appears that chaotic oscillations can successfully be distinguished from random oscillations by examining the appropriate higher order coherence.

ACKNOWLEDGMENTS

The ideas of and conversations with P. G. Vaidya and M. L. Anderson are gratefully acknowledged. Charles Pezeshki acknowledges the encouragement of E. H. Dowell. Charles Pezeshki's research is supported by a grant from Washington State University's OGRD program. Steve Elgar's research is supported by the Office of Naval Research (N00014-86-K-087) and the National Science Foundation (OCE-8612008). Signal processing computations were performed at the San Diego Supercomputer Center (supported by NSF).

REFERENCES

1. K. HASSLEMAN, W. MUNK and G. MACDONALD 1963 in *Time Series Analysis* (M. Rosenblatt, editor), 125-139, Bispectra of ocean waves. New York: John Wiley.
2. T. T. YEH and C. W. VAN ATTA 1973 *Journal of Fluid Mechanics* **58**, 233-261. Spectral transfer of scalar and velocity fields in heated-grid turbulence.
3. K. S. LII, M. ROSENBLATT and C. VAN ATTA 1976 *Journal of Fluid Mechanics* **77**, 45-62. Bispectral measurements in turbulence.
4. K. N. HELLAND, C. W. VAN ATTA and G. N. STEGUN 1977 *Journal of Fluid Mechanics* **79**, 337-359. Spectral energy transfer in high Reynolds number turbulence.
5. C. W. VAN ATTA 1979 *Physics of Fluids* **22**, 1440-1443. Inertial range bispectra in turbulence.
6. Y. C. KIM, J. M. BEALL, E. J. POWERS and R. W. MIKSAD 1980 *Physics of Fluids* **21**(8), 258-263. Bispectrum and nonlinear wave coupling.
7. R. MIKSAD, F. JONES and E. POWERS 1983 *Physics of Fluids* **26**, 1402-1409. Measurements of nonlinear interactions during natural transition of a symmetric wake.
8. C. RITZ, E. POWERS, R. MIKSAD and R. SOLIS 1988 *Physics of Fluids* **31**, 3577-3588. Nonlinear spectral dynamics of a transitioning flow.
9. D. CHOI, J. H. CHANG, R. STEARMAN and E. POWERS 1984 *Proceedings of the 2nd International Modal Analysis Conference* **II**, 3-12. Bispectral identification of nonlinear mode interactions.
10. T. SATO, K. SASAKI and Y. NAKAMURA 1977 *Journal of the Acoustical Society of America* **62**(2), 382-387. Real-time bispectral analysis of gear noise and its application to contactless diagnosis.
11. M. MILLER 1986 *Physical Review* **B34**, 6326-6333. Bispectral analysis of the driven Sine-Gordon chain.

12. C. L. NIKIAS and M. R. RAGHUVEER 1987 *Institute of Electrical and Electronic Engineers Proceedings* **75**(7), 869–891. Bispectrum estimation: A digital signal processing framework.
13. A. J. LICHTENBERG and M. A. LIEBERMAN 1983 *Regular and Stochastic Motion* New York: Springer-Verlag. see pp. 386–389.
14. J. B. THOMPSON and H. B. STEWART 1986 *Nonlinear Dynamics and Chaos.* New York: John Wiley see pp. 235–238.
15. E. H. DOWELL and C. PEZESHKI 1986 *American Society of Mechanical Engineers Journal of Applied Mechanics*, **53**(1), 5–9. On the understanding of chaos in Duffings equation including a comparison with experiment.
16. F. C. MOON and P. J. HOLMES 1979 *Journal of Sound and Vibration* **38**, 275–296. A magnetoelastic strange attractor.
17. N. H. PACKARD, J. P. CRUTCHFIELD, J. D. FARMER and R. S. SHAW 1980 *Physical Review Letters*, **45**(9), 712–715. Geometry from a time series.
18. P. GRASSBERGER and I. PROCACCIA 1983 *Physical Review Letters* **50**, 346–349. Characterization of strange attractors.
19. J. C. ROUX, R. H. SIMOYI and H. L. SWINNEY 1983 *Physics* **8D**, 257–266. Observation of a strange attractor.
20. P. GRASSBERGER and I. PROCACCIA 1983 *Physics* **9D**, 189–208. Measuring the Strangeness of strange attractors.
21. J. FARMER, E. OTT and J. YORKE 1983 *Physica* **7D**, 153–179. The dimension of chaotic attractors.
22. P. FREDERICKSON, J. KAPLAN, E. YORKE and J. YORKE 1983 *Journal of Differential Equations* **49**, 185–207. The Lyapunov dimension of strange attractors.
23. C. PEZESHKI and E. H. DOWELL 1989 *International Journal of Non-Linear Mechanics* **24**(2), 79–97. Generation and analysis of Lyapunov exponents for the buckled beam.
24. A. WOLF, J. B. SWIFT, H. L. SWINNEY and J. A. VASTANO 1985 *Physica* **16D**, 285–317. Determining Lyapunov exponents from a time series.
25. Y. C. KIM and E. J. POWERS 1979 *Institute of Electrical and Electronic Engineers Transactions on Plasma Science* **PS-7**(2), 120–131. Digital bispectral analysis and its applications to nonlinear wave interactions.
26. R. A. HAUBRICH 1965 *Journal of Geophysical Research* **70**, 1415–1427. Earth noises, 5 to 500 millicycles per second.
27. D. M. TANG and E. H. DOWELL 1988 *American Society of Mechanical Engineers Journal of Applied Mechanics* **55**(1), 190–196. On the threshold force for chaotic motions.
28. E. H. DOWELL and C. PEZESHKI 1988 *Journal of Sound and Vibration* **121**, 195–200. On necessary and sufficient conditions for chaos to occur in Duffing's equation: a heuristic approach.